EXPERIMENTAL DEMONSTRATION OF WAKEFIELD EFFECTS IN A 250 GHZ PLANAR DIAMOND ACCELERATING STRUCTURE*

S. Antipov#, C. Jing, P. Schoessow, S. Zuo, J. Butler and A. Kanareykin,
Euclid Techlabs LLC, Solon, OH 44139 USA
W. Gai, Argonne National Laboratory, Argonne, IL 60439 USA
M. Fedurin, K. Kusche and V. Yakimenko,
Brookhaven National Accelerator Laboratory, Upton, NY 11973 USA

Abstract

We have directly measured the mm-wave wake fields induced by subpicosecond, intense relativistic electron bunches in a diamond loaded accelerating structure via the dielectric wake-field acceleration mechanism. Fields produced by a leading drive beam were used to accelerate a trailing witness electron bunch which followed the driving bunch at an adjustable distance. The energy change of the witness bunch as a function of its separation from the drive bunch is a direct measurement of the wake potential.

INTRODUCTION

High gradient dielectric – loaded accelerating structures (DLA) have received significant attention in recent years [1-4]. Such devices are rather simple to fabricate. Typical examples would be a dielectric tube inserted into a conducting jacket or a rectangular waveguide loaded with dielectric plates. DLAs are compact; magnetic correctors in the form of a solenoid or series of quadrupoles can be placed around the structure. More importantly, dielectrics exhibit higher breakdown thresholds [2] and they are easily scalable to THz [2 - 4] and even higher frequencies where they have lower total structure losses compared to metals. Dielectric structures are also less sensitive to single bunch beam break-up (BBU) instabilities [5].

CVD (chemical vapor deposition) diamond has been proposed [6, 7] as a dielectric material for wakefield DLA structures [1-3]. It has a very low microwave loss tangent, the highest available thermal diffusivity and a high RF breakdown field. The large secondary emission from the as manufactured CVD diamond surface can be dramatically suppressed by diamond surface dehydrogenation or oxidation [8]. CVD diamond has already been routinely used on an industrial basis for large-diameter output windows of high power gyrotrons, and is being produced industrially in reasonable quantities.

Here we present results from experimental studies of a rectangular waveguide loaded with polycrystalline CVD diamond plates as an accelerating structure. It should be noted especially that in this experiment [13] diamond was for the first time used as a loading material for a wakefield dielectric based accelerating structure.

*Work supported by the Department of Energy SBIR program under Contract #DE-FG02-08ER85033.
#s.antipov@euclidtechlabs.com

EXPERIMENT

The general experimental methodology is the following (Fig. 1). A pair of beams is generated: a high charge drive beam, followed by a smaller witness beam at a variable distance *d*. The beams pass through the wakefield structure. The drive beam generates a wake there and the witness beam is accelerated or decelerated depending on the delay between the two beams. We record the witness beam energy change, ΔE as a function of *d*.

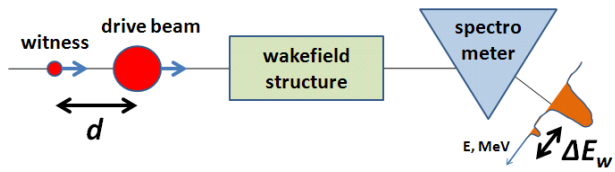

Figure 1: General scheme of the experiment: the separation between the drive and the witness beam is changed and compared with the change of the witness beam energy on the spectrometer.

A short witness beam effectively samples the field left behind the drive beam. This idea is also used to map transverse wakes [14]. The original direct measurements of wakefields were performed at Argonne [1] in the 10 GHz frequency range. In this paper we present direct wakefield measurement at 250 GHz performed at Accelerator Test Facility (ATF) of Brookhaven National Laboratory [13].

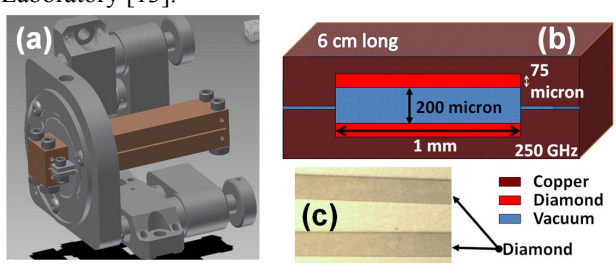

Figure 2: a) structure mounted on a positioning holder; b) structure dimensions; c) photo of diamond after the experiment exhibiting no visible damage.

In the experiment we used 75 micron thick polycrystalline diamond plates loaded in a 6 cm long waveguide (Fig. 2). The beam gap was 200 microns (Fig. 2(b). This structure yields a wakefield dominated by a TM_{11} – like mode with 1200 micron wavelength (0.25

THz). The ATF drive beam is very short and also excites higher order modes, hence the wake is not a pure sine wave (see Fig. 5).

The subpicosecond drive and witness beams are produced by the technique described in [9]. A beam accelerated off-crest hence having a linear energy chirp (the head of the beam having lower energy than the tail) passes through a dogleg – a dispersionless translating section that consists of two bending dipoles whose bend angles are equal in magnitude but opposite in sign. Focusing optics are located between the dipoles. A mask is placed between the dogleg dipoles where the beam transverse size is dominated by the correlated energy spread. After the second dipole magnet the transverse pattern introduced by the mask becomes the longitudinal charge density distribution. In our case the mask was motorized and allowed creation of a drive beam followed by a witness beam at a variable delay.

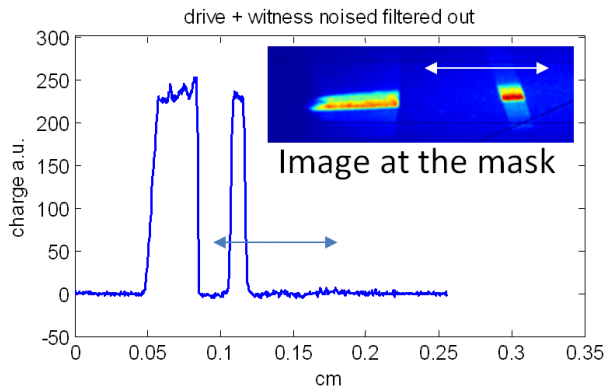

Figure 3: Extraction of the experimental current profile for data processing.

The mask pattern and the image of the beam on the phosphor screen immediately after the mask is correlated with beam's resulting longitudinal distribution after the second set of dipole magnets. Therefore the image of the beam after the mask can be calibrated to determine the resulting beam's longitudinal distribution. This calibration is done via coherent transition radiation (CTR) interferometry. In this technique two test beamlets are created by the mask and recorded on a phosphor screen after the mask. In particular the distance between the beamlets is measured on the phosphor screen. After the second dipole the distance (along z) between these two beamlets is measured by interferometric manipulation of the transition radiation signal which the beamlets emit passing through a thin CTR foil. Wavelengths longer than the beams are emitted coherently and carry information about the bunch lengths [10, 11]. Transition radiation is sent to an interferometer and the signal is recorded by a helium-cooled bolometer [4, 9]. From this measurement the distance between beamlets was determined and the phosphor screen image was calibrated. In our experiment we measured the drive beam longitudinal size to be 320 microns, and the witness beam was about 100 microns long. Figure 3 shows the image on the phosphor screen after the mask and the longitudinal current distribution obtained by this measurement and used in the theoretical wakefield computation. In this case we neglected the dispersion of the beam while it was being delivered to the experimental area where the diamond structure was installed. The dispersion effect was estimated by simulation (the program MAD (Methodical Accelerator Design) [12]) to be less than 5%.

It is worth noting that the shaped beam still carries a linear energy chirp; in our case the head (drive) beam having higher energy than the witness beam (tail). Because of that when distance between the drive beam and the witness beam is being increased the new witness beam has higher energy then the previous witness beam due to the linear energy chirp required for this beam shaping technique. It is essential to calibrate this effect out, because the wakefield mapping procedure relies on the measurement of witness beam energy gain or loss as a function of the drive – witness beam delay.

From CTR interferometry calibration we obtained the longitudinal current distribution in the drive beam. The transverse beam distribution was obtained from the image on the phosphor screen directly in front of the structure. We fitted the recorded transverse profile by a gaussian distribution with σ_x = 50 µm, σ_y = 350 µm. The longitudinal wakefield produced by a beam with this current distribution was numerically calculated and compared with the experimental results.

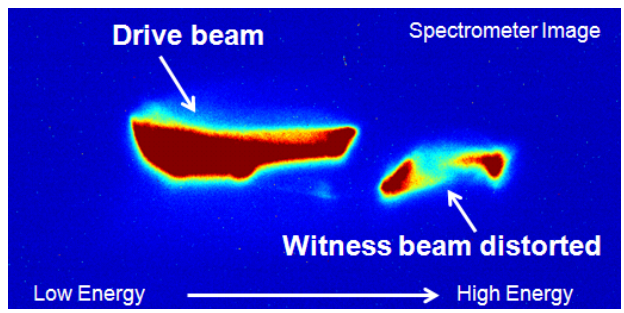

Figure 4: Spectrometer image shows the witness beam breaking up in two beamlets.

Because of the relatively large longitudinal size of the witness beam its head and tail sample different fields. In most cases this results in an increase in the witness beam energy spread. The witness beam can split in two as well (Fig. 4) when the high energy part of the beam is accelerated, while the lower energy part is decelerated. We traced the centroid of the witness beam when post-processing the results (Fig. 5).

The spectrometer image is calibrated by varying the current in the spectrometer magnet. The relative change in witness beam energy depending on the drive – witness separation is measured on the spectrometer. Compared to the beam energy, when it does not go through the structure, we observe energy gain and loss in the interval from -0.6 to +0.65 MeV for the witness beam following a drive beam through the DLA structure. This yields a 10.8 MV/m gradient for a 6 cm structure. The measurement accuracy was limited by the spectrometer resolution (σ =

ISBN 978-3-95450-115-1

0.028 MeV), estimated using the sharpest features obtained on the spectrometer by measuring the FWHM (full width half maximum) and dividing it by 2.355 to obtain the equivalent Gaussian width. Beam stability was also crucial for the relative energy measurement. The observed jitter of the spectrometer image corresponded to 0.015 MeV. Finally, the tracking centroid of the witness beam could be determined with accuracy equal to the standard deviation of its energy spread. Figure 5 shows the measured energy change (diamonds) as a function of drive – witness separation with error bars.

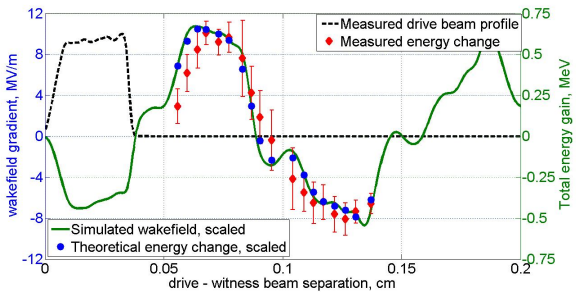

Figure 5: Energy gain of the witness beam as a function of separation from the drive beam. The shape of the experimentally mapped wake (diamonds) agrees well with the theoretical (scaled) prediction (circles) based on the wakefield (solid line) calculated for the drive beam current distribution (dashed line).

SUMMARY AND PLANS

In conclusion, we have directly measured wakefield acceleration / deceleration in a diamond loaded dielectric accelerating structure.

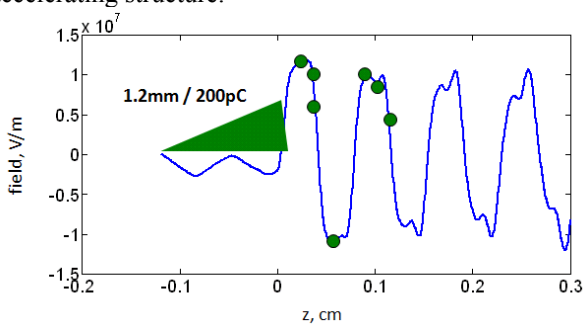

Figure 6: Planned experiment: enhanced transformer ratio (TR) with a triangular-shaped drive beam. The decelerating field inside the drive is about 4 times lower than the accelerating field for the witness beam (implying TR≈4).

The witness beam was accelerated in the field produced by a subpicosecond drive beam. By sweeping the separation between the drive beam and the witness beam and energy measurements of the witness beam the 0.25 THz frequency wakefield was directly sampled at the scale of about one wavelength.

We plan to follow up this experiment with a similar one, involving a triangular current profile in the drive beam (see Fig. 6). This beam configuration yields a so-called enhanced transformer ratio [15], TR>2: TR = (maximum energy gain of the witness bunch) / (maximum energy loss of the drive bunch). It is desirable to have a high transformer ratio to accelerate the witness bunch to higher energies given the limited energy of the drive bunch.

REFERENCES

[1] W. Gai, P. Schoessow, B. Cole, R. Konecny, J. Norem, J. Rosenzweig, and J. Simpson, Phys. Rev. Lett. 61, 2756 (1988)

[2] M. C. Thompson, H. Badakov, A. M. Cook, J. B. Rosenzweig, R. Tikhoplav, G. Travish, I. Blumenfeld, M. J. Hogan, R. Ischebeck, N. Kirby et al., Phys. Rev. Lett. 100 (2008) 214801.

[3] A. M. Cook, R. Tikhoplav, S. Y. Tochitsky, G. Travish, O. B. Williams, and J. B. Rosenzweig, Phys. Rev. Lett. 103 (2009) 095003.

[4] G. Andonian, O. Williams, X. Wei, P. Niknejadi, E. Hemsing, J. B. Rosenzweig, P. Muggli, M. Babzien, M. Fedurin, K. Kusche et al., Appl. Phys. Lett. 98 (2011) 202901.

[5] P. Schoessow, A. Kanareykin, C. Jing, A. Kustov, A. Altmark, J. G. Power, and W. Gai, Proceedings AAC-2008, AIP Conference Proceedings 1086 (2009) 404.

[6] A. Kanareykin, P. Schoessow, M. Conde, C. Jing, J.G. Power and W. Gai, Proc. Europ. Part. Accel. Conf. EPAC 2006, p. 2460 (2006).

[7] S. Antipov, C. Jing, A. Kanareykin, P. Schoessow, M. Conde, W. Gai, S. Doran, J. G. Power, Z. Yusof, AIP Conf. Proc, Particle Accelerator Conference, New York, p. 2074 (2011).

[8] F. Maier, J. Ristein, L. Ley, Phys. Rev. B 64 (2001) 165411.

[9] P. Muggli, V. Yakimenko, M. Babzien, E. Kallos, and K. P. Kusche, Phys. Rev. Lett. 101 (2008) 054801.

[10] D. C. Nguyen and B. E. Carlsten, Nucl. Instrum. Methods Phys. Res., Sect. A 375 (1996) 597.

[11] M. Ter-Mikaelian, *High-Energy Electromagnetic Processes in Condensed Media* (Wiley-Interscience, New York, 1972).

[12] H. Grote, C. Iselin, The MAD program (methodical accelerator design): version 8.10; user reference manual (Geneva, CERN, 1993).

[13] S. Antipov, C. Jing, A. Kanareykin, J.E. Butler, V. Yakimenko, M. Fedurin, K. Kusche, and W. Gai, Appl. Phys. Lett. 100 (2012) 132910.

[14] W. Wuensch, SAREC review meeting, 2012, http://indico.cern.ch/getFile.py/access?contribId=0&resId=1&materialId=slides&confId=144201

[15] K.L. Bane, P. Chen, P.B. Wilson, SLAC-PUB-3662, Apr., 1985.